JOURNAL OF THE SOUTHEASTERN ASSOCIATION FOR RESEARCH IN ASTRONOMY, **2**, 6-9, 2008 MAY 1

MICROLENSING OF DUSTY STELLAR ENVELOPES BY A POINT MASS LENS

CHRISTINA BUNKER[1]
Department of Physics and Astronomy, SUNY Stony Brook, Stony Brook, NY 11790
AND
RICHARD IGNACE
Department of Physics, Astronomy, and Geology, East Tennessee State University, Johnson City, TN 37614

ABSTRACT

By modeling gravitational microlensing events, it is possible to study the structure of lensed sources from variable flux amplifications as the event progresses. In fact, it is quite the converse scenario of eclipse mapping. We consider microlensing events with a point mass lens and a spherically symmetric finite source that has a dusty envelope. Our goal is to model these events and understand how to map the circumstellar envelope intensity profile from a study of the variable spectral data.

Subject headings: techniques: microlensing — ISM: dust

1. INTRODUCTION

Microlensing of finite sources is a relatively new method we can use to study stellar sources, their atmospheres, and their extended envelopes. Monochromatic light curves from finite sources with constant surface brightness were discussed by Witt and Mao (1994). Valls-Gabaud (1996, 1998) predicted that one could discover properties of the stellar atmosphere through lensing light curves. He studied systematic chromatic effects as well as limb darkening spectroscopic effects through microlensing. Gould (2001) discusses how stellar sources can be resolved during binary lens caustic crossings.

Microlensing of emission line profiles from circumstellar envelopes was first discussed by Ignace and Hendry (1998). They showed how variable flux amplification in line profiles could be related to the flow structure in the circumstellar envelope. Bryce, Ignace, and Hendry (2002) extended the study through a consideration of binary caustic crossings events.

In this paper we address the following: In section 2, we discuss the basics of microlensing and calculate the amplification for a few special cases. We briefly cover circumstellar mass loss and dust formation in section 3 as relevant to our modeling. We then discuss our results from our microlensing simulations in section 5, and in section 6, end with our conclusions.

2. MICROLENSING BASICS

Gravitational lensing refers to how gravity bends light from a straight line trajectory. Einstein predicted that mass could deflect light from the straight path it would typically follow. He also calculated the angular deflection of light at the limb of the sun, which Eddington verified observationally during a solar eclipse in 1919.

A consequence of gravitational lensing is that multiple images are generated from a single background source. This is observed when a massive cluster of galaxies or even a single galaxy is nearly aligned with a far more distance source, such as a quasar. In the case of nearly perfect alignment an Einstein Ring will be seen; however, it is more often the case that multiple images are produced in the form of distorted arcs of light. More details about the mathematics of gravitational lensing and applications to astrophysics can be found in Schneider, Ehlers, & Falco (1992), Mollerach & Roulet (2002), and Petters, Levine, & Wambsganss (2001).

2.1. *Point Source and Point Mass Lens*

The amplification of a point source lensed by a point mass lens is of the form

$$A = \frac{p^2 + 2R_E^2}{p\sqrt{p^2 + 4R_E^2}} \tag{1}$$

where p is the impact parameter of the event, and R_E is the Einstein Radius. The amplification A describes the relative enhancement in source brightness as a function of proximity between the projected lens and source positions. For large separations, $p \gg R_E$, the amplification is unity, indicating that there is no lensing effect. However, when $p \ll R_E$, one finds that $A \propto p^{-1}$ becomes quite large. In fact, it diverges, which as we shall see means the point source assumption is no longer valid.

The Einstein radius (R_E) represents a characteristic distance in the source plane in which microlensing begins to be significant. Its value is related to mass and distance via

$$R_E = \sqrt{\frac{4GM_L}{c^2}\frac{(D_S - D_L)D_L}{D_S}} \tag{2}$$

where G is the gravitational constant, M_L is the mass of the lens, c is the speed of light, D_S is the distance to the source, and D_L is the distance to the lens. To give a sense of scale, we normalize the expression as follows:

$$R_E = 2.9AU \left(\frac{M_L}{M_\odot}\right)^{\frac{1}{2}} \left[\frac{(D_S - D_L)D_S}{D_L}\right]^{\frac{1}{2}} \tag{3}$$

where M_L is in solar masses, and all of the distances are in kpcs. Then R_E is typically of the scale of a few AU.

2.2. *Finite Source and Point Mass Lens*

Of course in reality, stars are not point sources. They have some finite area that emits flux. Consequently, if a lens passes to close to the limb of a star or in fact transits the star, the event

[1] Southeastern Association for Research in Astronomy (SARA) NSF-REU Summer Intern
Electronic address: christina.bunker@gmail.com; ignace@etsu.edu

can no longer be modeled in a point source approximation. The expression for the source amplification now involves an integral over the projected source size. The new amplification $\tilde{A}$ is given by:

$$\tilde{A} = \frac{\int A(s) I(p,\alpha)\, p\, dp\, d\alpha}{\int I(p,\alpha)\, p\, dp\, d\alpha} \tag{4}$$

where $A(s)$ is the amplification as a function of the angular separation between the lens and an element of the source, s is any radius defined in the lens plane, $I(p,\alpha)$ is the intensity of light which is function of the radial coordinate in the source plane p, and α the angular coordinate in the source plane. When the impact parameter is large, in other words the lens and the source are far apart, the amplification will approach unity. When the two objects move into alignment, the impact parameter approaches zero, and the amplification given in equation 1 becomes linear in the Einstein radius.

When the source and the lens are directly aligned with the observer, the geometry in the integral of equation 3 is greatly simplified because $s = p$. Figure 1 shows the geometry for this situation. Taking the intensity as constant over the surface of the star $I(p) = I_*$, we find the total amplification $\tilde{A}$ by integrating equation 3 over its' surface.

$$\tilde{A} = \frac{\sqrt{4R_E^2 + R_S^2}}{R_S} \tag{5}$$

This amplification approaches $2R_E/R_S$ when $R_E \gg R_S$. For $R_E \ll R_S$ the amplification reduces to unity.

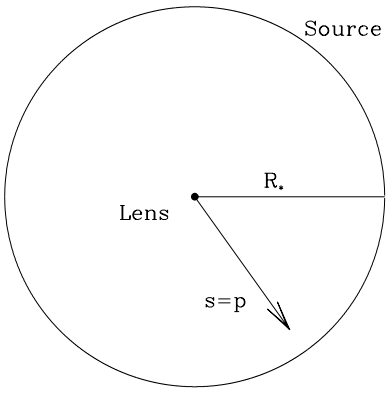

FIG. 1.— A finite source is shown behind a point mass lens. The radius of the source is R_S.

If the intensity were not constant, but varied for example, as $I(p) = p/R_S$ the amplification would then be

$$\tilde{A} = \frac{\left[x^{\frac{3}{2}} - 6R_E^2 x^{\frac{1}{2}} + 4R_E^3\right]}{R_S^3} \tag{6}$$

where $x = R_S^2 + 4R_E^2$. Here when $R_E \gg R_S$ we find with a second order approximation that the amplification approaches $3R_E/2R_S$. On the other hand, in the limit that $R_E \ll R_S$, the amplification drops to unity, as expected.

In general, the value used for the stellar radius depends on the wavelength of observation, namely $R_* = R_\lambda$. The star can appear larger or smaller accordingly. It can be seen in equations 5 and 6 that this will result in an amplification factor that is wavelength-dependent, an effect that we shall refer to as "chromatic."

These simple cases illustrate what to expect from more complicated microlensing models. They show us that the amplification will be sensitive to different intensity profiles from the source. If the star and lens are not perfectly aligned with the observer, the geometry of the integral in equation 3 will become much more complicated. Microlensing events amplify the flux intensity that varies over a finite star, thus, it is a useful technique to gain knowledge about the source.

3. THE CIRCUMSTELLAR MODEL

Mass is continually being lost from stars to their surrounding environment through winds. The mass loss rate is described by the continuity relation, which for spherical symmetry is

$$\dot{M} = 4\pi r^2 \rho v \tag{7}$$

From this the density profile in flow is

$$\rho = \frac{\dot{M}}{4\pi r^2 v(r)} \propto r^{-2} \tag{8}$$

$\dot{M}$ is the mass loss rate that we assume to be a constant, ρ is the density, r is the radius out from the star, and v is the outward velocity the material. For our simulations we take the wind velocity to be fixed so that the density follows an inverse square law (following Simmons et al. 2002).

Because the stellar atmosphere is so hot, mass loss from the star generally is in the form of gas. Dust grains are not able to form until the wind has cooled to a temperature of approximately 1500K. For this reason, we refer to the region void of dust around the star, as a cavity. Surrounding the cavity is where we find the dust formation, and this is referred to as the envelope. The dust heats up by absorbing stellar radiation and it re-emits photons in the infrared part of the spectrum.

Our models are concerned with hybrid spectra consisting of radiation from a stellar atmosphere for a red giant and also the emission from a dusty circumstellar envelope. However, these components form over vastly different spatial regions, in particular because the stellar atmosphere is too hot for dust to exist.

4. MONTE CARLO SIMULATIONS

We use a Monte Carlo routine written by Jon Bjorkman at the University of Toledo for our microlensing simulations. It uses a random number generator and opacity sampling to simulate radiation transfer under the assumption of radiative equilibrium (Bjorkman & Wood 2001). The spectra do show fluctuations owing to the random number approach, and their quality are governed by Poisson statitics. We used 50 million photons to achieve low statistical errors in the spectral models. Throughout the simulations, we always assume a density profile for the circumstellar envelope of $\rho \propto r^{-2}$

The key control parameters considered are the radius of the dust shell in relation to the star radius (R_{dust}), the optical depth (τ), the Einstein radius(R_E), and a Kurucz fixed star model atmosphere with a temperature of 3500 K (Kurucz 1992). The Monte Carlo routine uses the user defined inputs to calculate flux intensity at various distances from the lens as a function of wavelength, as well as the linear polarization.

5. RESULTS

Our simulations show that it is possible to learn about structure of dusty envelopes through microlensing events. Studies of monochromatic models illustrate how the flux at a particular wavelength of light will change through the course of a lensing event, while chromatic simulations allow us to investigate flux amplifications over the whole spectrum. We focus our analysis on the effects of dust that occur in the infrared part of the spectrum.

5.1. *Monochromatic*

Figure 2 displays model light curves from microlensing of a star and circumstellar envelope with only electron scattering. Models of dusty envelopes are presented in the following section. Here we want to highlight the effect of how optical depth in the envelope can change the source size with consequence for the lensing light curve by considering only a gray scattering opacity. The intensity changes as the lens crosses the source. The amplification seen depends on the effective radius. Large optical depth leads to essentially to a large pseudo-photosphere. This represents the same effect as having different sizes at different wavelength, the effect discussed in section 2.2.

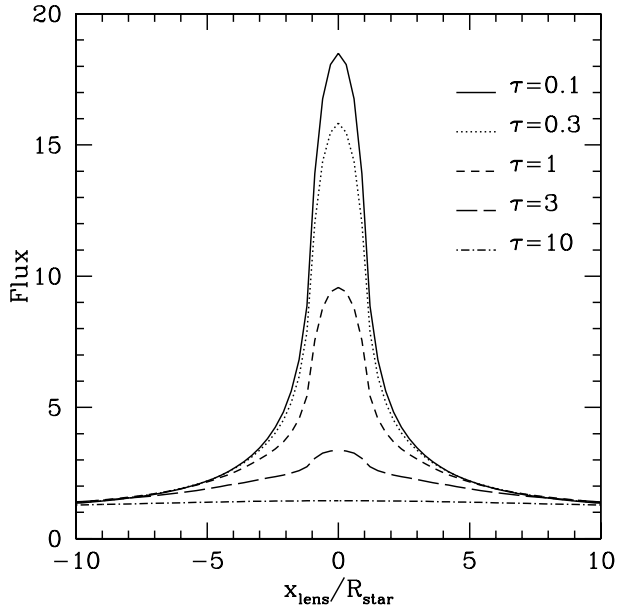

FIG. 2.— Monochromatic modeled light curves, Thompson scattering varied optical depths, R_{dust} = 3 and R_E = 10 for a star

5.2. *Chromatic*

It is possible to study the multi-wavelength effects on models of microlensing events to map the stellar atmosphere as well as the dusty envelope. Models of chromatic flux from a microlensing event of a finite source by a point mass lens are shown in figures 3, 4, and 5. In these figures we study the effects of varied dust shell radii, Einstein radii, and optical depths. Light curves are overplotted to show how the wavelength of the light will affect the flux for varied lens-source positions. In all three figures we find agreement in that the maximum flux due to the event increases when the two objects are closer to alignment.

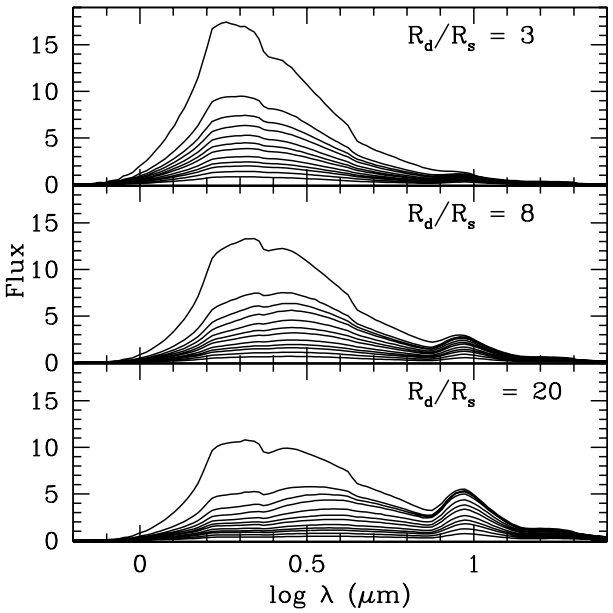

FIG. 3.— Light curves for models where a star with a dusty envelope is lensed. It is shown on a logscale plot of wavelength to show chromatic effects. Curves with larger maximum intensity correspond to smaller lens impact parameters. For all R_E = 10, τ = 10

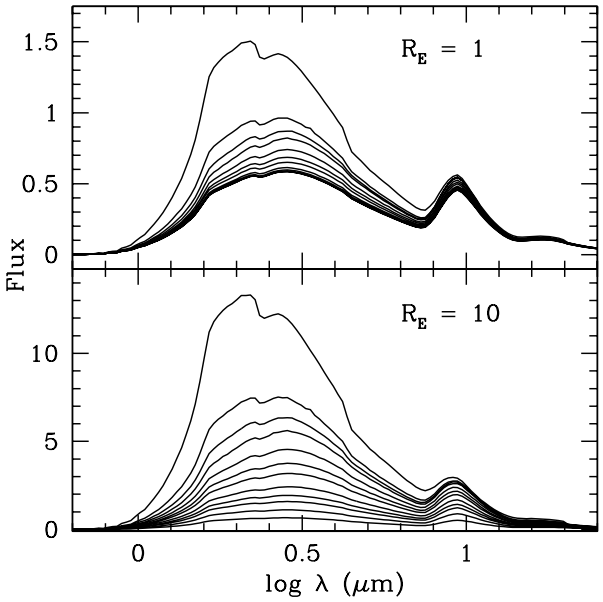

FIG. 4.— Light curves for models where a star with a dusty envelope is lensed. It is shown on a logscale plot of wavelenghth to show chromatic effects. Curves with larger maximum intensity correspond to when the lens and source are closer together. For all R_{dust} = 8 and τ = 10

- The model of the chromatic microlensing of a finite star by a point mass lens shown in figure 3 has fixed parameters of $R_E = 10R_S$ and $\tau = 10$ to emphasize the effects from a varied dust shell radius. Typically a star emits a spectrum similar to a blackbody, however when there is a dust shell surrounding the star second maximum appears in the infrared. When the dust shell radius increases, the infrared peak flux does also.

- The model shown in figure 4 has a fixed $R_{dust} = 8R_S$ and $\tau = 10$ maximize the effects from varied Einstein

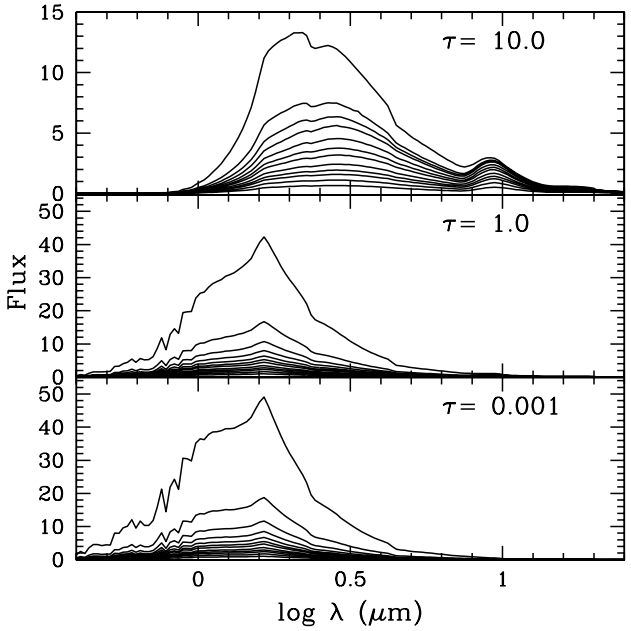

FIG. 5.— Light curves for models where a star with a dusty envelope is lensed. It is shown on a logscale plot of wavelenghth to show chromatic effects. Curves with larger maximum intensity correspond to when the lens and source are closer together. For all R_{dust} = 8 and R_E = 10

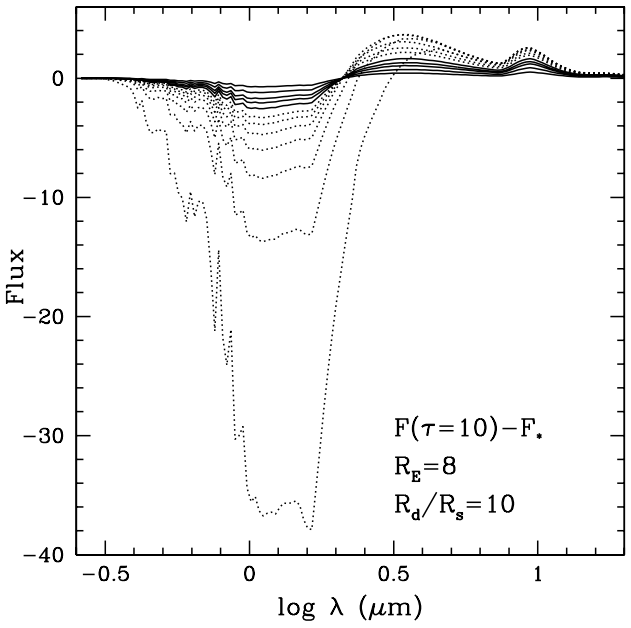

FIG. 6.— Flux of models where a star with a dusty envelope is lensed minus the flux of a model of only a star. The logscale plot shows the chromatic effects.

radii. It is easily seen, that the larger Einstein radius causes increased amplification of both the flux from the star and the dust no matter what the impact parameter. We note that when the lens-source separation is large the amplification is nearly constant with wavelength, a reflection of the fact that the source size is much larger than the Einstein radius.

- The model shown in figure 5 has fixed parameters of $R_E = 10R_S$ and $R_{dust} = 8R_S$ highlighting the effects from variations in optical depth. When the optical depth is small we find, as expected, the result to be essentially the same as lensing a star with no dust. As the optical depth increases the peak flux values decrease significantly due to the opaqueness of the atmosphere. The effects of the dust are much more visible with optical depths greater than unity and we can observe the second peak in in the infrared part of the spectrum.

- Figure 6 is an illustration constructed from two seperate models. We subtracted the spectrum from the lensing of only the star from a spectrum with the same parameters except for having a high optical depth. It is possible to see where photons have been absorbed out of the radiation from the star and where some of those were reemitted by the dust at a longer wavelength. Dotted lines correspond to positions when the lens and the source are closer to alignment and the solid lines are when they are further apart. This was just as expected because the lensing becomes stronger when the observer is closer in alignment with the source and lens.

6. CONCLUSIONS

We constructed models of specta to use in microlensing event simulations where the source is finite and surrounded by a dusty envelope. We studied the effects of altering the properties of the dust envelope in terms of its cavity radius, its optical depth, and the lens Einstein radius. As we expected, we found that when the lensing is strong, wavelength dependent effects seen in the amplified spectra allow one to probe the dust emission, which is relevant for observations of lensed red giant stars and their winds.

We are grateful to Jon Bjorkman for providing us with his Monte Carlo code. This project was funded by a partnership between the National Science Foundation (NSF AST-0552798), Research Experiences for Undergraduates (REU), and the Department of Defense (DoD) ASSURE (Awards to Stimulate and Support Undergraduate Research Experiences) programs.

REFERENCES

jorkman, J., Wood, K., 2001, ApJ, 554, 615
Bryce H.M., Ignace R., Hendry M.A., 2003, A&A, 401, 339
Gould A., 2001, PASP, 113, 903
Ignace R., Hendry M.A., 1999, A&A, 341, 201
urucz, R.L., 1992, in IAU Symposium 149, The Stellar Populations of Galaxies, ed. B. Barbuy & A. Renzini (Dordrecht: Kluwer), 225
Mollerach S., Roulet E., 2002, Gravitational Lensing and Microlensing
Petters A.O., Levine H., Wambsganss J., 2001, Singularity Theory and Gravitational Lensing, (Boston: Birkhäuser)
Schneider P., Ehlers J., Falco E.E., 1992, Gravitational Lenses, (Berlin: Springer-Verlag)
immons, J., Bjorkman, J., Ignace, R., Coleman, I., 2002, MNRAS, 336, 501
Valls-Gabaud D., 1996, in Kochanek C.S., Hewitt J.N., eds, Proc. IAU Symp. 173. Astrophysical Applications of Gravitational Lensing. Kluwer,Dordrecht, p.237
Valls-Gabaud D., 1998, MNRAS, 294, 747
Witt H.J., Mao S., 1994 ,ApJ, 430, 505